Flight Test Coursework

Spaceflight
UFMFCH-15-3

Dr. Chris Toomer
Dr. Pritesh Narayan

Faculty of Environment and Technology
Department of Engineering, Design and Mathematics

Jake Bamford – 13002405

Melissa Eberle – 13024498

Samuel Lupton – 14003356

Yuichiro Toyama – 13023630

Abstract

The objective of this assignment was to compare flight test data to theoretical values obtained using computational software such as MATLAB/Simulink. This would aid in obtaining a better understanding of the process of aircraft flight testing. There were two aircraft choices for the investigation, Jetstream 31 or Eurostar EV97. As the majority of the group went on a trip to Cranfield University to take part in a Jetstream 31 flight test course, this aircraft was chosen.

MATLAB code was generated for each dynamic flight mode followed by simulations via Simulink. A set of state-space control matrices for the lateral and longitudinal motion was used by the model to simulate the response of the Jetstream 31 to control inputs from aileron, rudder, elevator and throttle. Results obtained from this were compared with those extracted from real flight test data from Cranfield using graphs and numerical methods.

The Simulink models were successfully created, modelling short period, phugoid, and Dutch roll oscillations. They successfully demonstrate the correct motions of the aircraft, however the accuracy of the models can be improved.

Table of Contents

List of Figures

List of Table

List of abbreviations

IFR	Instrument Flight Rules
VFR	Visual Flight Rules
POH	Pilots Operating Handbook
AOA	Angle of Attack
GPS	Global Positioning System
IRS	Inertial Reference System
ILS	Instrument Landing System
CSV	Comma Separated Value
TAS	True Airspeed
EAS	Equivalent Airspeed
SPPO	Short Period Pitching Oscillation

1. Introduction

The aircraft investigated in this paper is the Jetstream 31. It is a small twin-turboprop commercial airliner by British Aerospace which received its airworthiness accreditation in 1982. It is a limited aircraft as only 386 aircraft were manufactured. It offers space for two pilots and up to 18 passengers. Its wing span is 15.8 meters and the length of the fuselage is 14.4 meters. The maximum take-off weight of the Jetstream 31 is about 7059kg. Each of its turboprop produces 701 kW which enables a range of 1260 km with a cruise speed of 426km/h. The Jetstream 31 can operate in Visual Flight Rules (VFR) as well as in Instrument Flight Rules (IVR). [1]

Figure 1: Jetstream 31

1.1 Flight Testing

Flight testing is a branch of aeronautical engineering that develops and collects data during a flight of an aircraft or an atmospheric test of launch vehicles. It uses the data collected to analyse the aerodynamic flight characteristics of the vehicle in order to validate the design and to make sure it clears the safety criteria. [2]

The flight test phase during an aircraft's development accomplishes two major tasks. The first is to find and fix any design problems in the aircraft. The second is to verify and document the aircraft's capabilities for government certification. A flight test can range from the test of a single new system up to a complete development and certification of a new aircraft. Due to this, depending on the aircraft or system and the sector it belongs to, this can take a few weeks up to several years.

Flight testing is a vital part of any aircraft's development and therefore it needs to be properly documented. Without correct documentation, the test will only produce a collection of anecdotes and random numbers unless it is processed appropriately.

Due to the advancement in computational abilities, a range of aircraft designs can be tested to determine the optimal configurations. However, for this to perform correctly, the flight dynamics model has to link with the aircraft in flight. This means, the models built based on Newton's laws of motion, it requires the aircraft design information such as drag, lift, weight, stability, various coefficients and derivatives are utilized. Flight test data was recorded during specific flight manoeuvres in order to estimate the behaviour of the Jetstream 31. To ensure the future use of these data, they had to be recorded and organized.

1.2 Aims

The task as a group was to extract flight test data collected and compare with results obtained from a flight simulation model developed on Simulink. The Simulink data was collected by simulating the dynamic flight modes in the longitudinal and lateral direction inherent in the particular aircraft. Flight test data will be collected in a variety of aircraft and environmental conditions which include altitude and location, temperature and humidity. State-space control matrices for lateral and longitudinal models would be developed with the use of applicable data and formulae. MATLAB code is created and dynamic models simulated via Simulink.

For the models to be accurate, all relevant variables and parameters which would determine the aircrafts geometry and flight performance were needed. Some could be found from internet searches and calculated from flight test data but more complex values needed to be extracted from more specific sources such as "Flight Stability and Automatic Control" by R. Nelson and "A Simulation Model of the NFLC Jetstream 31" by A. Cooke.

It is important to see if there is a correlation between the data collected and data created through statistical analysis of the aircraft flight modes. This will show if there are any outliers or incorrect data. Following this, comparisons can be made between flight data results and Simulink model results. They can also be compared against information available in the POH.

2. Literature Review

2.1 Longitudinal Static Stability

The longitudinal handling qualities of the aircraft involve motion in the pitching moment. If the aircraft is to demonstrate stability, any change in the angle of attack must produce a response which will try to restore the aircraft to its original state. For example, if there is a nose up disturbance (AOA positive), it will produce a response where the nose pitches down (negative AOA). As a results, the aircraft will try to return to its original state and AOA.

Assuming the aircraft is stable, a simple test could be performed to show the change in pitching moment relative to changes in the AOA. The aircraft will be held in a steady state

where the pitching moments will equal 0. This will result in the aerodynamic pitching moments produced by the aircraft and moments due to the pilot's control to the elevator to be balanced.

$$0 = M_\alpha \alpha + M_\eta \eta \quad (1)$$

M_α is the aerodymamic pitching moment derivative of the aircraft and α is the AOA. M_η is the aerodynamic pitching moment derivative of the elevator and η is the elevator deflection. [3]

2.2 Longitudinal Dynamic Stability

There are two types of longitudinal dynamic stability, short period and long period (phugoid). Short period and phugoid can be thought as a gradual interchange of potential and kinetic energy about the altitude and airspeed equilibrium which can be seen in figure(?). It shows that phugoid is determined by changes in altitude but maintains a constant AOA but short period is determined by changes in AOA but maintains a constant airspeed. [4]

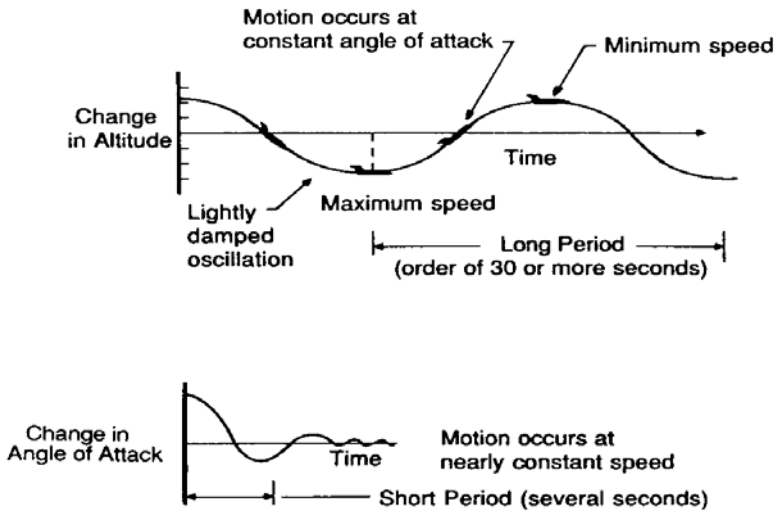

Figure 2: Diagram showing the differences in phugoid and short period [4]

2.2.1 Short Period Pitching Oscillation

Short period is the most important dynamic mode and consists of a damped oscillation about the aircraft pitch axis. Whenever the aircraft is disturbed from its pitch equilibrium, the short period is excited and starts oscillating where the principle values are pitch rate and AOA. Normally the frequency of the mode is 0.5 to 2 Hz which is within the natural frequency of the pilot. This is why it is vital the short period mode is well damped and without it being so, severe handling problems could arise. [3]

2.2.2 Short Period Pitching Oscillation approximation

Short period mode motion can be approximated by assuming the rate of change in velocity is small and dropping the X force equation. The longitudinal state-space equations become:

$$\begin{bmatrix}\Delta\dot{w}\\ \Delta\dot{q}\end{bmatrix} = \begin{bmatrix}Z_w & u_0\\ M_w + M_{\dot{w}}Z_w & M_q + M_{\dot{w}}u_0\end{bmatrix}\begin{bmatrix}\Delta w\\ \Delta q\end{bmatrix} \tag{2}$$

The above equation can be written in terms of the AOA by using the relationship $\Delta\alpha = \frac{\Delta w}{u_0}$ which gives the state equations for the short period approximation as:

$$\begin{bmatrix}\Delta\dot{\alpha}\\ \Delta\dot{q}\end{bmatrix} = \begin{bmatrix}\frac{Z_\alpha}{u_0} & 1\\ M_\alpha + M_{\dot{\alpha}}\frac{Z_\alpha}{u_0} & M_q + M_{\dot{\alpha}}\end{bmatrix}\begin{bmatrix}\Delta\alpha\\ \Delta q\end{bmatrix} \tag{3}$$

The eigenvalues of the state equation can be determined by solving for $|\lambda\mathbf{I} - \boldsymbol{A}| = 0$ and expanded to give:

$$\begin{vmatrix}\lambda - \frac{Z_\alpha}{u_0} & -1\\ -M_\alpha - M_{\dot{\alpha}}\frac{Z_\alpha}{u_0} & \lambda - \left(M_q + M_{\dot{\alpha}}\right)\end{vmatrix} = 0 \tag{4}$$

$$\lambda^2 - \left(M_q + M_{\dot{\alpha}} + \frac{Z_\alpha}{u_0}\right)\lambda + M_q\frac{Z_\alpha}{u_0} - M_\alpha = 0 \tag{5}$$

Frequency and damping ratio can be expressed as:

$$\omega_{n_{sp}} = \sqrt{\frac{Z_\alpha M_q}{u_0} - M_\alpha} \qquad \zeta_{sp} = -\frac{M_q + M_{\dot{\alpha}} + \frac{Z_\alpha}{u_0}}{2\omega_{n_{sp}}} \tag{6}$$

2.2.3 Phugoid Oscillation

Phugoid oscillation is most commonly seen as having a lightly damped and low frequency oscillation in airspeed which pairs with height. Whenever the aircraft is disturbed from trim speed, the phugoid mode manifests itself as a sinusoidal oscillation in which the main values are pitch attitude and change in airspeed. The period for phugoid (long period) is longer compared to short period hence its name normally in the band of 40-100 seconds. The low damping is mainly caused by the rate of change in drag with speed change. The higher period allows the pilot to control the aircraft even if it is unstable making it a rather undemanding task.

2.2.4 Phugoid Oscillation approximation

Phugoid approximations can be made by neglecting pitching moment equation and assume the change in AOA is zero.

$$\Delta\alpha = \frac{\Delta w}{u_0} \qquad \Delta\alpha = 0 \rightarrow \Delta w = 0 \tag{7}$$

With these assumptions made, the homogenous longitudinal state equations become:

$$\begin{bmatrix} \Delta\dot{u} \\ \Delta\dot{\theta} \end{bmatrix} = \begin{bmatrix} X_u & -g \\ \frac{-Z_u}{u_0} & 0 \end{bmatrix} \begin{bmatrix} \Delta u \\ \theta \end{bmatrix} \tag{8}$$

The eigenvalues of the phugoid approximation can be obtained by solving the equation below which expands to give:

$$\begin{vmatrix} \lambda - X_u & g \\ \frac{Z_u}{u_0} & \lambda \end{vmatrix} = 0 \qquad \lambda^2 - X_u\lambda - \frac{Z_u}{u_0} = 0 \tag{9}$$

Frequency and damping ratio can be expressed as:

$$\omega_{n_p} = \sqrt{\frac{-Z_u g}{u_0}} \qquad \zeta_p = \frac{-X_u}{2\omega_{n_p}} \tag{10}$$

Neglecting compressibility effects, the frequency and damping ratios for the phugoid mode can be estimated using the following equation.

$$\omega_{n_p} = \sqrt{2}\frac{g}{u_0} \qquad \zeta_p = \frac{1}{\sqrt{2}}\frac{1}{L/D} \tag{11}$$

2.3 Lateral Dynamic Stability

There are 3 types of lateral modes which are Dutch roll mode, roll subsidence mode and spiral mode. They differ to longitudinal by the direction of the motion which include rolling and yawing motions. The motions in these axes are almost always coupled together with the other modes therefore are generally discussed at lateral directional modes.

2.3.1 Dutch Roll Mode

The Dutch roll mode is an oscillatory motion about the yaw axis where the principal variables are sideslip angle and yaw rate whilst the aircraft maintains a straight flight path. Fundamentally the mode is the same as the short period but in the other direction. One characteristic which differs from short period is that the sinusoidal change in sideslip cause a similar change to the rolling moment (dihedral effect). This makes the aircraft oscillate in roll and yaw. [3]

2.3.2 Roll (Subsidence) Mode

The roll mode is an exponential change in roll rate therefore it is not oscillatory and is first order. This means, when there is change in roll it will gain a new roll exponentially. This causes exponential lag especially in aileron response. The mode is almost entirely due to the viscous damping effect of the wing and therefore always present and stabilising in its effect.

For the pilot, the mode appears as a lag in roll control and if the time constant is too large, then the control becomes sluggish. For the Jetstream, the time constant is small enough where the lag is almost unnoticeable.

2.3.3 Spiral Mode

The spiral mode is also non oscillatory and shows exponential convergence or divergence in roll attitude and causes a divergent spiral descent when unstable. The time constant is usually large, normally 40 seconds therefore the mode is slow to develop.

When roll attitude is disturbed, the lift vector will also rotate which could cause some sideslip. If sideslip is the same direction as roll, the dihedral effect will produce a moment which reduces bank angle, but the fin will produce yaw moment the same direction as roll. All the moments are small hence the long time constant. The stability depends on the relative magnitudes of the dihedral and weathercock effect.

It being a long period mode, it does not affect short term handling too much and when stable has no risks. However, when unstable, the aircraft diverges from level flight when left alone. This poses a threat when visibility is poor and has unnoticeable motions cues with it.

3. Methodology

3.1 Flight test data extraction

A mentioned above, flight test data is just a series of random numbers which have no meaning unless it is properly tabulated and formatted into a graph. When on board the Jetstream 31, the pilot will inform the passengers which mode they would execute and how they would achieve it. The pilots also mentioned why it is important to test the particular mode and how it applies to the real world.

On board the rear of the aircraft was the instrumentation system which consists of conditioning units, power supplies, inertial reference unit and a data acquisition system. There are also sensors and transducers located around the aircraft to measure control surface deflections, applied control forces, aircraft attitudes, AOA and sideslip, rate of rotation and acceleration, differential static pressure and navigation sensors such as GPS, IRS and ILS.

Transducer outputs are converted in the signal conditioning unit and data acquisition system into physical units for display and recording. This data was made available after the trip to Cranfield through Blackboard. The data was supplied as a CSV file which allowed us to manipulate in any way or form through Excel. All the relevant graphs are given in the results section and explained what they mean.

3.1.1 Short Period Pitching Oscillation

The values for short period given in the .csv file were time, elevator deflection, AOA, pitch attitude, pitch rate and yawing moment lateral to the body. To show the short period response, a graph showing the elevator deflection and AOA over time was needed. This would show how the AOA attack changes when an impulse is applied to the elevator. Another useful graph would be the pitch rate over time as this will show how the impulse affects how quickly it changes the pitch attitude of the aircraft.

3.1.2 Phugoid Oscillation

The values for phugoid mode were time, elevator deflection, pitch angle, airspeed and altitude. Graphs for each variable needed to be plotted over time as there are all interconnected. Hence they are presented below in a column to show how one variable are linked to another. The time variable is lined up to show this easier and which is why only the bottom graph horizontal axis is labelled.

3.1.3 Dutch Roll Mode

The variable included for the Dutch roll mode were time, rudder deflection, sideslip, yaw rate, roll rate, lateral acceleration, roll angle and TAS. Graphs were plotted for rudder deflection,

sideslip, yaw rate and roll rate against time. Similar to the phugoid oscillation, the 4 graphs were plotted in a column to show the link between each variable. Roll angle and TAS were not plotted as the roll motion could be better seen from the roll rate graph. TAS was ignored as although there was a change in speed, the range was only 7 knots and it was measured to 1 knot therefore not giving a smooth graph but rather a block one.

3.1.4 Roll (Subsidence) Mode

The variables produced from the roll mode were time, aileron deflection, bank angle, roll rate, sideslip and yawing moment lateral to the body. Graphs were plotted for aileron deflection and roll rate to best represent the roll mode response. Since aileron deflection and roll rate are inversely proportional to each other, the graph should be almost symmetrical along the horizontal axis. Another graph was plotted to show the bank attitude of the aircraft to show how the ailerons affect the bank angle. Although there were some sideslip and yawing moment, there were very little (sideslip ranged from -1 to 3.5 degrees) and since it was a test on the roll axis, graphs were not plotted.

3.1.5 Spiral Mode

The final values from the CSV file were for the spiral mode which included variables of time, roll angle, altitude, airspeed and aileron deflection. Graphs were plotted for all variables and displayed as a column to see the correlation.

3.2 MATLAB and Simulink

In order to effectively simulate a Jetstream aircraft a Simulink Program was created based on a basic template provided on Blackboard. The final Simulink model is structured around six MATLAB Codes. The first code is a simple launch code which, when run, launches the Simulink File. When the Simulink file is then run it utilises three MATLAB codes to initialise the system.

The file named 'AircraftConfig.m' contains the variables that carry the physical attributes of the Jetstream. Some of these values were located in the POH, others were calculated from the flight test data and the remaining were calculated from these two subsets. These variables are separated from the rest of the code to aim in the readability of the code.

The calculations pertaining to the state space models are coded in the 'Longitudinal_And_Lateral.m'. Two separate state space models are used to simulate flight, one is for longitudinal motion and the other lateral. The Longitudinal model processes all movement in the XZ plane: airspeed, vertical speed, pitch rate, and pitch angle. The Lateral model processes all movement in the XY plane: sideslip, roll rate, yaw, and roll angle. The code first loads the atmospheric data from an external array and splits this information into individual arrays for each variable. The program then launches 'AircraftConfig.m' to create the required data from the Jetstream. Once the information is loaded, these values for the longitudinal matrices A and B followed by the lateral matrices A and B are calculated. These values are then inputted into the matrices and two additional matrices, C and D are created for each model. C is an identity matrix of size 4 and D is zero matrix size [4, 2]. Each state space model is then created with their respective A, B, C, and D matrices. The code then describes the starting position of the aircraft stating, for example, any initial velocity, angle of attack or roll.

$$\begin{bmatrix} \Delta\dot{u} \\ \Delta\dot{w} \\ \Delta\dot{q} \\ \Delta\dot{\theta} \end{bmatrix} = \begin{bmatrix} X_u & X_w & 0 & -g \\ Z_u & Z_w & u_0 & 0 \\ M_u + M_{\dot{w}}Z_u & M_w + M_{\dot{w}}Z_w & M_q + M_{\dot{w}}u_0 & 0 \\ 0 & 0 & 1 & 0 \end{bmatrix} \begin{bmatrix} \Delta u \\ \Delta w \\ \Delta q \\ \Delta\theta \end{bmatrix} + \begin{bmatrix} X_{\delta_e} & X_{\delta_T} \\ Z_{\delta_e} & Z_{\delta_T} \\ M_{\delta_e} + M_{\dot{w}}Z_{\delta_e} & M_{\delta_T} + M_{\dot{w}}Z_{\delta_T} \\ 0 & 0 \end{bmatrix} \begin{bmatrix} \delta_e \\ \delta_T \end{bmatrix}$$

Figure 3: Longitudinal Matrix

$$\begin{bmatrix} \Delta\dot{v} \\ \Delta\dot{p} \\ \Delta\dot{r} \\ \Delta\dot{\phi} \end{bmatrix} = \begin{bmatrix} Y_v & Y_p & -(u_0 - Y_r) & g\cos\theta_0 \\ L_v & L_p & L_r & 0 \\ N_v & N_p & N_r & 0 \\ 0 & 1 & 0 & 0 \end{bmatrix} \begin{bmatrix} \Delta v \\ \Delta p \\ \Delta r \\ \Delta\phi \end{bmatrix} + \begin{bmatrix} 0 & \frac{Y_{\delta_r}}{u_0} \\ L_{\delta_a} & L_{\delta_r} \\ N_{\delta_a} & N_{\delta_r} \\ 0 & 0 \end{bmatrix} \begin{bmatrix} \delta_a \\ \delta_r \end{bmatrix}$$

Figure 4: Lateral Matrix

The ‘Pre_3D_Visualisation’ code is provided and is used to load the image of the aircraft that will be used to show the simulated movements. The code was altered slightly to use an image of a ‘80jet’ as it was a closer fit to the Jetstream that the default image. The ‘Body fixed to Inertial’ code was also provided in the default package. It is used to rotated the values of the aircraft from the state space models to the appropriate position so that all forces are directed at the correct angle. To accomplish this a rotation matrix is utilised. The ‘3D Visualisation’ takes the data that the rotation matrix and uses it to update the visualization of the aircraft. This code was also provided in the default code package.

The folder also includes a code named ‘PeriodRoots’ this section of code is designed to be run from the command window once the state space models have been created. It is used to find the characteristics of the short and long period oscillations and is taken from an example in the lecture notes.

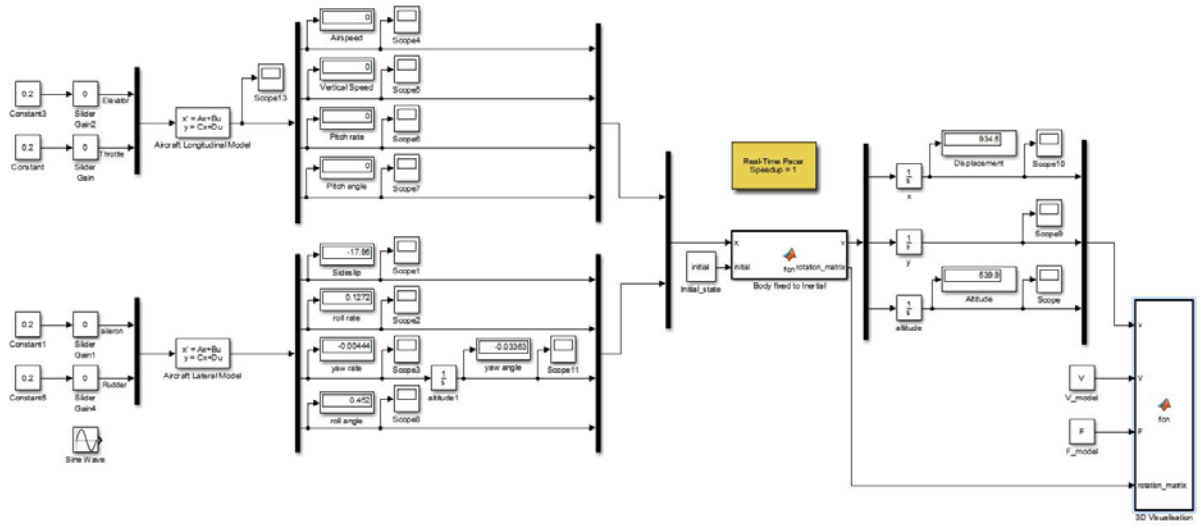

Figure 5: Simulink model designed for Jetstream 31

4. Results

4.1 Flight Test Results

Various flight modes were carried out during the flight test on board the Jetstream 31. This would test the dynamic stability for both the longitudinal and lateral directions. The on board computer recorded values for varying properties over a time. These results were later made available so relevant graphs could be generated so they could be checked to see if the relevant responses could be seen from the individual flight modes.

4.1.1 Short Period Pitching Oscillation

To test the short period pitching oscillation, the aircraft was initially at trim to maintain constant height and speed. Then a short duration disturbance was applied to the pitch by giving an impulse to the elevator. This action sets the aircraft at a new AOA by the time the elevator returns to its original position. The graph below shows that the AOA returns to its original angle in a short amount of time after the impulse in the elevator. The aircraft is flying in a steady condition until 5.6 seconds where the elevator is moved. By 6 seconds, the elevator is stationary and the AOA is increased by about 2.4 degrees from the original. The AOA is back to its original after 1.6 seconds since the elevator impulse. This response shows the short period dynamics which returns the AOA towards its original angle.

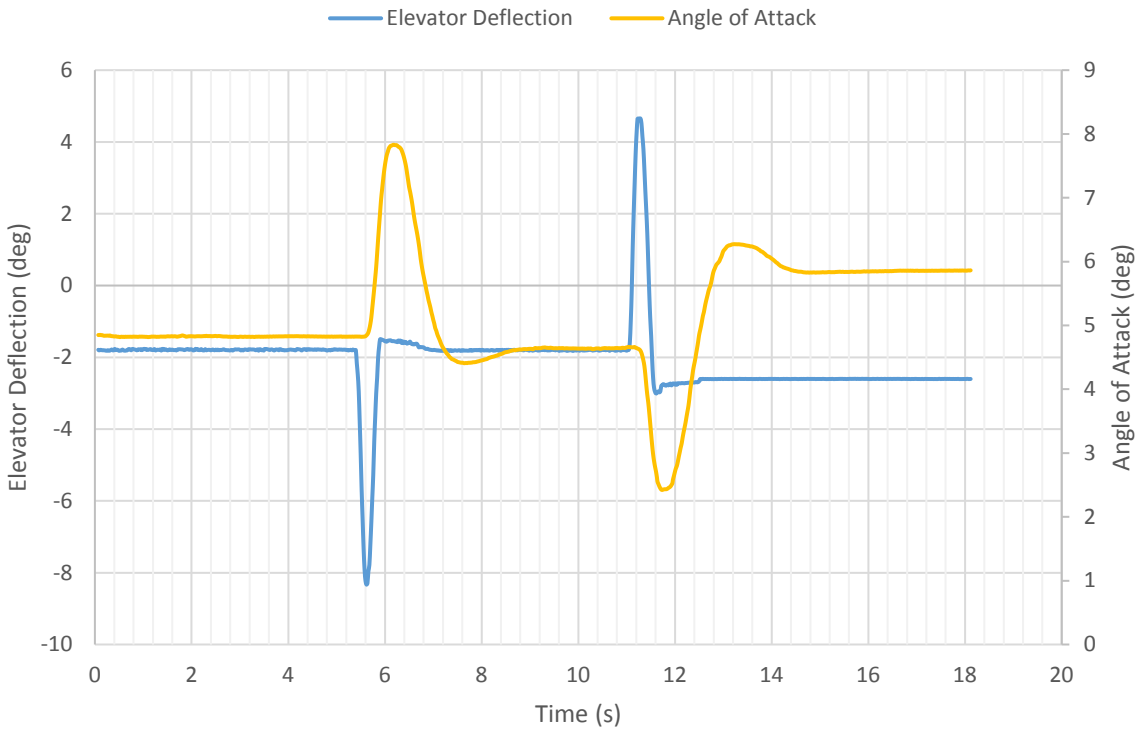

Figure 6: Graph showing SPPO response

The graph below shows the change in pitch rate over time. It can be seen that the pitch rate increases at the same time there is a change in the AOA and decreases back to its original when the AOA decreases. This is expected as elevator deflection, AOA and pitch rate are correlated. Angle of attack and pitch rate should show a directly proportional trend.

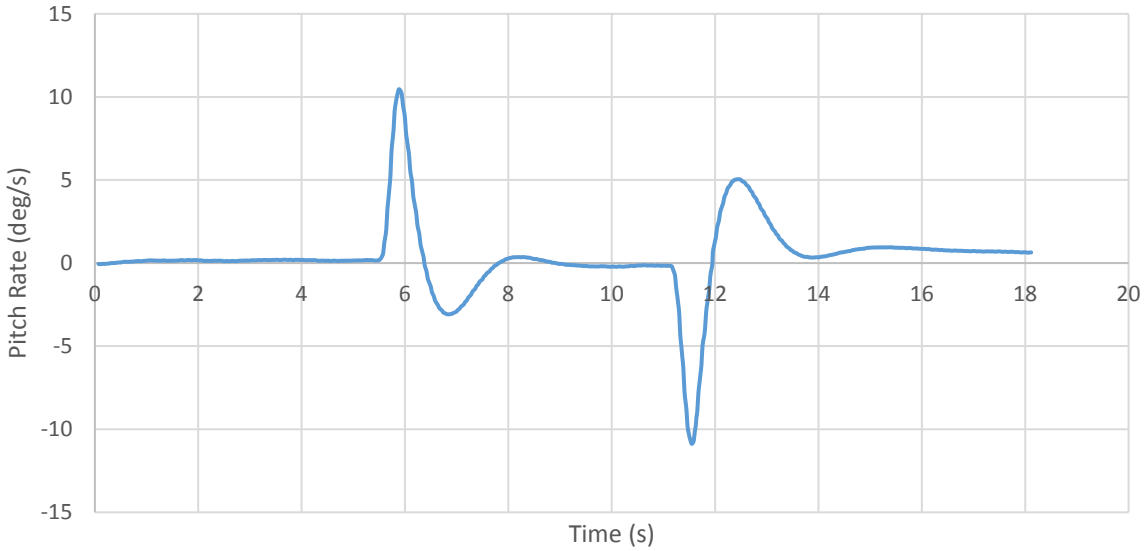

Figure 7: Graph showing pitch rate change during SPPO

4.1.2 Phugoid Oscillation

To test the phugoid mode, a gentle change in elevator was applied to change the pitch attitude and airspeed. When the speed has diverged sufficiently, the elevator is released to trim. During the recovery to its trimmed datum flight condition, the aircraft will overshoot the trim speed and execute a phugoid oscillation demonstrating poor damping which can be shown in the graphs below.

A change in elevator will also give the short period mode however this was minimised by the gentle movements applied to the elevator. Any transient would have died away before the phugoid has developed fully. This is the main difference between short period and phugoid.

The graph below shows the elevator was gently pulled back to pitch the aircraft in a nose up position and reduce speed. The elevator was released at approximately 28 seconds where the aircraft immediately starts to pitch nose down and airspeed increases. From this point, the elevator is held fixed and phugoid oscillations occur. The graph shows the oscillation period is roughly 50 seconds.

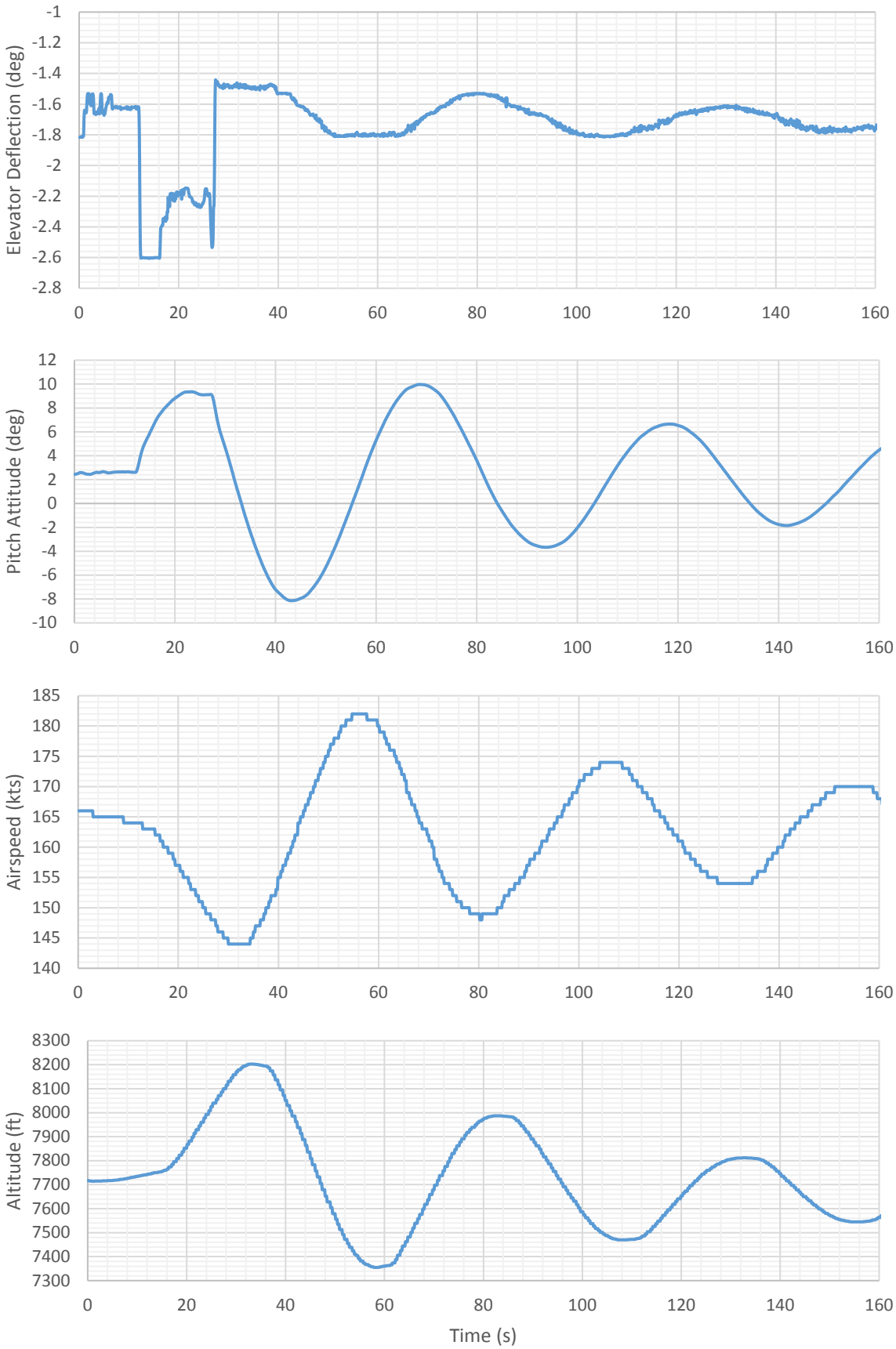

Figure 8: Graphs showing the Phugoid mode response

4.1.3 Dutch Roll

To test the Dutch roll, the aircraft is setup straight with wings level. The Dutch roll is activated by disturbing the yaw by moving the rudder in a sinusoidal manner at a frequency approximately equal to the mode. This will give a close symmetrical displacement in both sideslip and yaw rate which can be seen in the graphs below.

The graph shows that the aircraft was flying straight until there was a disturbance made to the rudder just after the 25 second mark. The rudder was moving left and right which caused sideslip, change in yaw and roll. It can be seen from the graphs that the sideslip, yaw rate and roll rate has approximately the same frequency (roughly 3 seconds) as the movement of the rudder from left to right.

Although the Dutch roll involves changes to the rudder which normally directly affect the yaw, due to the dihedral shape of the wings on the aircraft, there is change in roll as well. It can be seen that the magnitude of the Dutch roll increased until the rudder was released until the 40 second mark. The following oscillatory nature shows the poor damping of the Jetstream Dutch roll.

4.1.4 Roll (Subsidence) Mode

To test the roll mode, the aircraft is usually set up with 20 degrees of bank. The mode is activated by applying a small step displacement to the ailerons. Following the deflection in the ailerons, the aircraft rapidly acquires a steady roll rate after a short exponential rise which is determined by the mode time constant. After the bank angle has reached approximately 30 degrees in the opposite direction the aileron is centred to stop the rolling. A larger step displacement to before is applied to the ailerons in the opposite direction. Each aileron displacement changes the roll rate exponentially to a steady value.

From the graph below, it can be seen that the roll rate is close to 0 when there is no aileron deflection. However, at the 5.2 second mark, the ailerons are deflected negatively by approximately 7 degrees which as a result gives an exponential growth to the roll rate. The step increase in the aileron deflection can also be seen where first it was 7 degrees but the next was approximately 8 degrees.

The other graph shows the bank angle caused by the roll mode. It can be seen that the bank angle starts approximately at -20 degrees which was how the aircraft was set before the roll manoeuvre. It then increases just after the ailerons have been deflected to 30 degrees in the opposite direction. It stays there until the next step in aileron deflection.

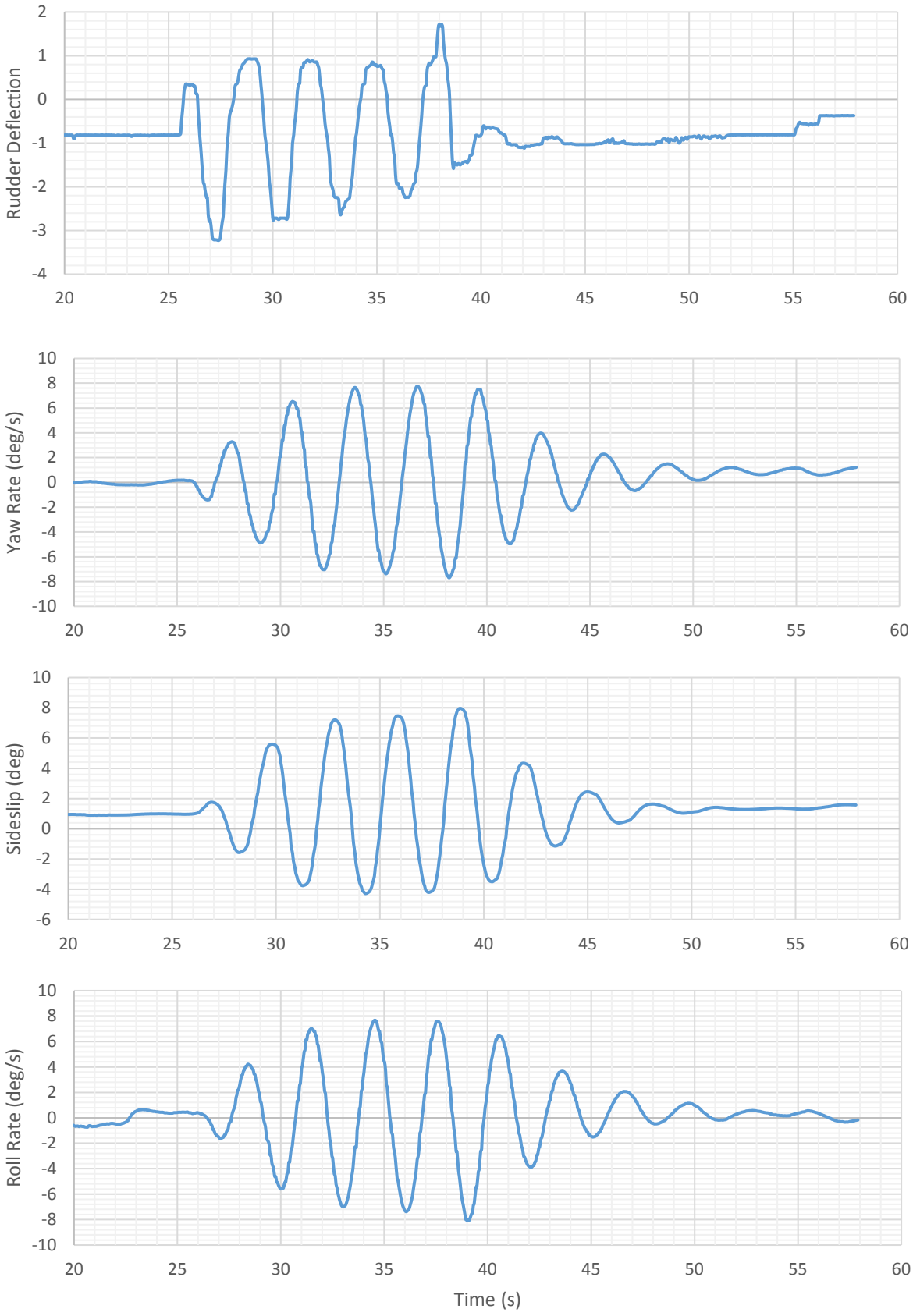

Figure 9: Graphs showing the Dutch Roll response

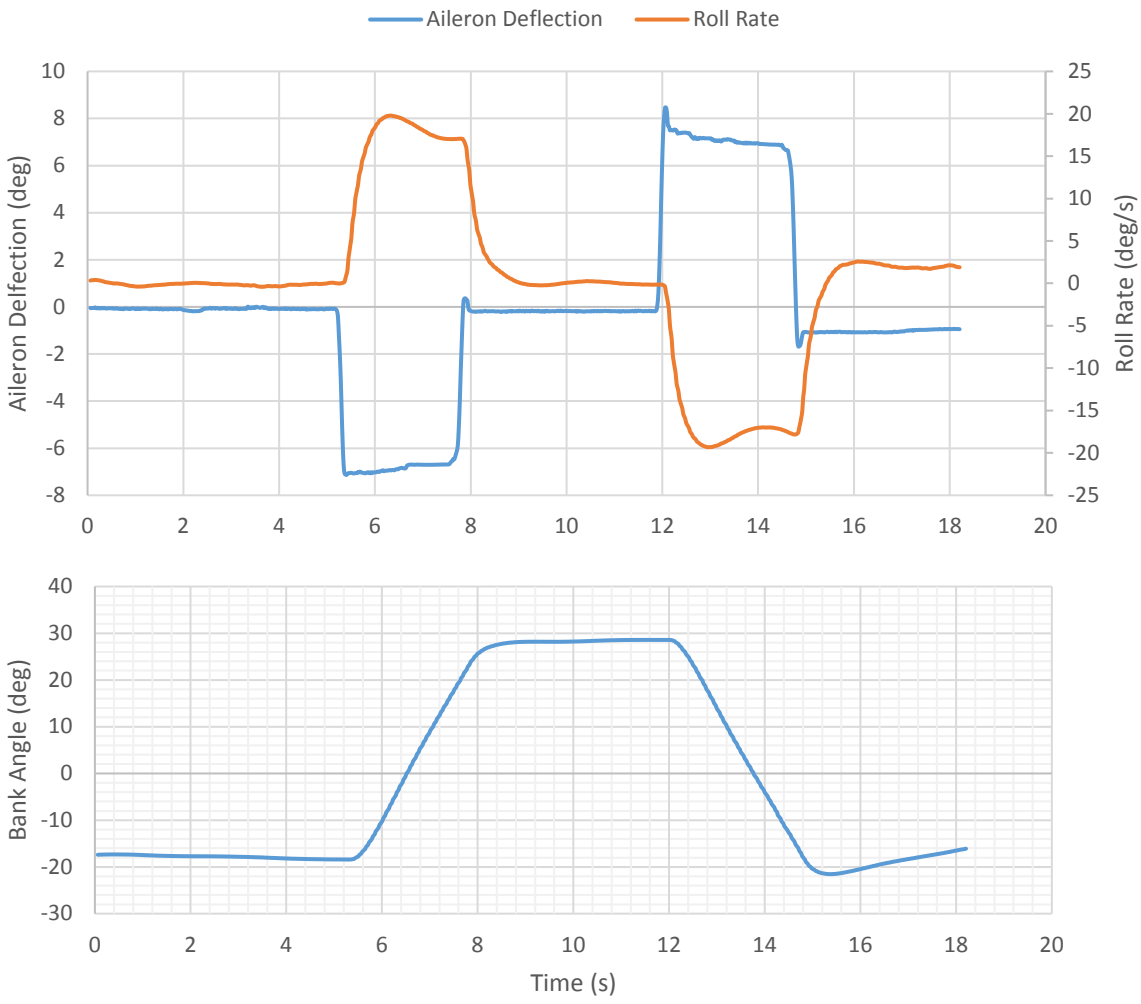

Figure 10: Graphs showing the Roll mode response

4.1.5 Spiral Mode

To carry out the spiral mode, first the aircraft is set up with 20 degrees of bank and then the controls released. When the spiral mode Is neutral, there will be no change in bank angle. However, if the mode is unstable the aircraft will start to diverge exponentially. The vertical stabiliser will keep the sideslip to a minimum but as a result the nose of the aircraft starts to fall increasingly further below the horizon which gives the spiral descent if left unchecked.

From the graphs above, it can be seen that the aircraft was flying level then set to a bank angle of -20 degrees at approximately the 14 second mark. It is also flying steady with an approximate altitude of 7500 ft and airspeed of 140 knots. The controls are released at 14 seconds and the bank angle slowly increases which indicates the spiral mode. This consequently decreases the altitude and increases the airspeed which can also be seen from the graphs. The spiral mode was put to a halt by levelling the aircraft near the 92 second mark.

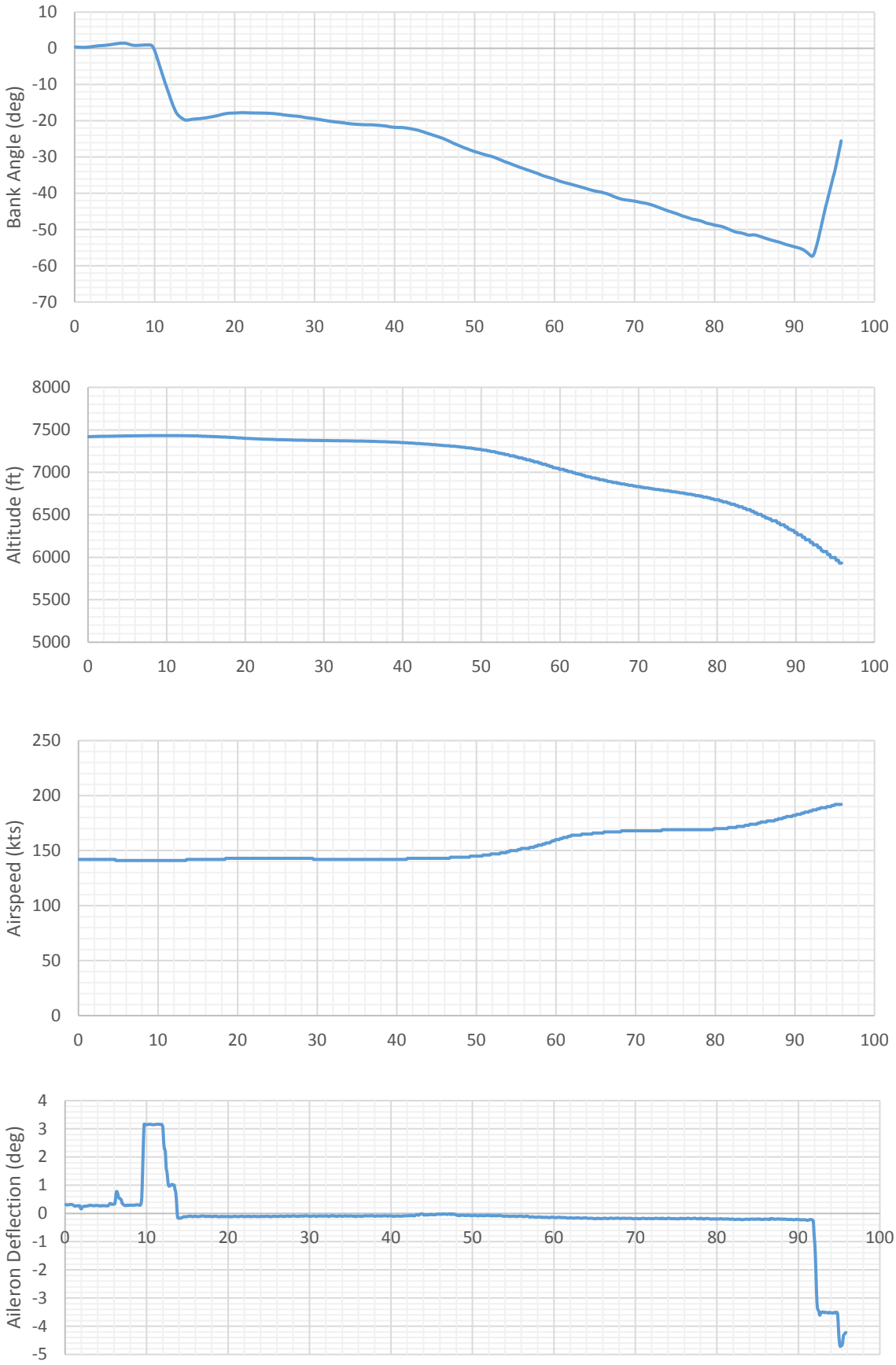

Figure 11: Graphs showing Spiral mode response

4.1 Simulink Results

After several test runs to confirm the MATLAB code and Simulink models were working to a sufficient accuracy, the relevant runs were completed to generate appropriate graphs. SPPO, phugoid and Dutch Roll produced encouraging graphs however, the roll mode and spiral mode were unsuccessful possibly due to the difficulty in emulating the specific manoeuvre through Simulink.

4.1.1 Short Period Pitching Oscillation

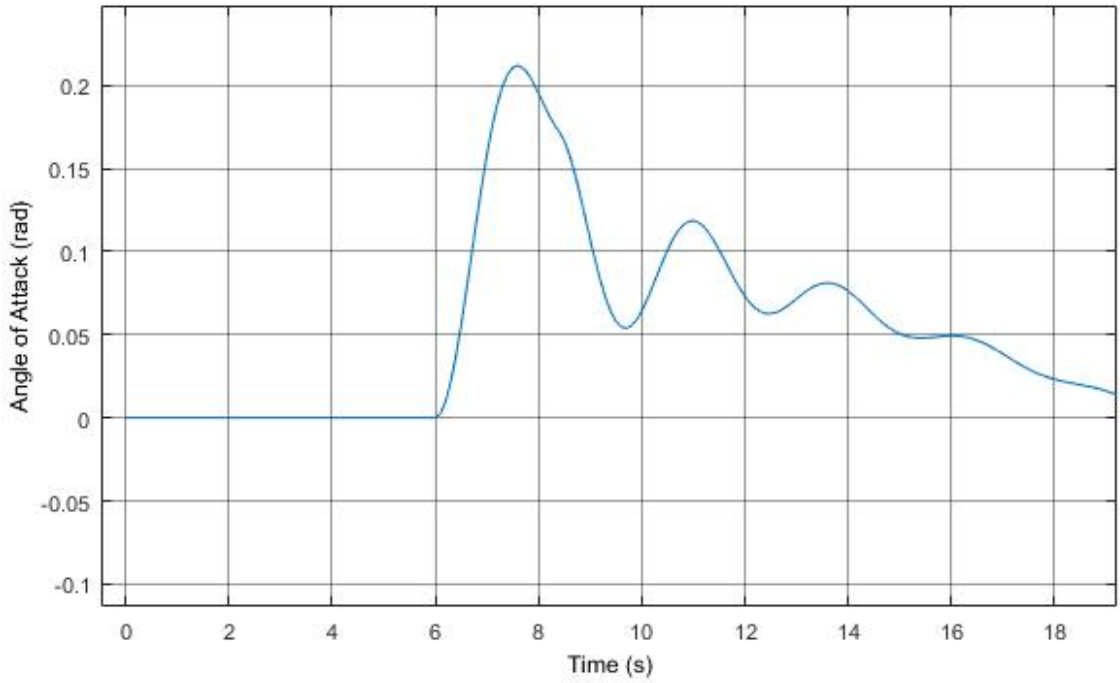

Figure 12: Graph showing change in AOA over time.

The above graph shows the response from the SPPO mode simulated on Simulink. It clearly shows the AOA is changing over a very short period of time. The y axis labelled AOA is in radians as this was the unit which was used in the MATLAB code. The graph shows the AOA increases a little over 0.2 radians (approx. 11 degrees) in nearly 1.7 seconds. This is slightly higher than the flight test data but it is within an acceptable range. This could be due to Simulink unable to account for the atmosphere accurately. This means the atmosphere of the real data created more drag slowing the increase in AOA whereas Simulink was unable to accurately represent this.

There is also a clear sign of damping which is good as this is also what happened seen from flight test data and is the expected behaviour.

4.1.2 Phugoid Oscillation

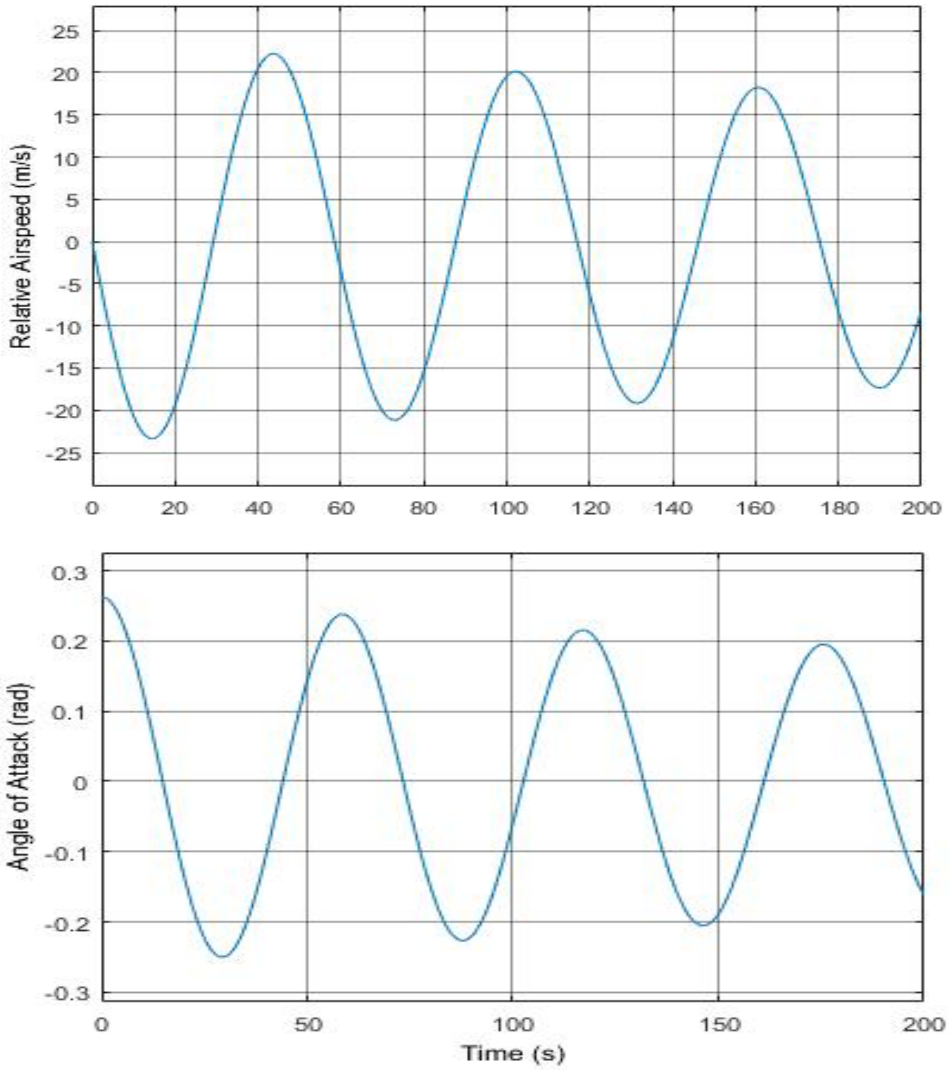

Figure 13: Graph showing phugoid response from Simulink

The results from Simulink for phugoid were very promising especially for airspeed. It was not possible to simulate the release of the stick therefore the aircraft was initially set with a specific AOA then controlled to how the pitch attitude would finish. Therefore, the exact movement of the elevator is not included in the simulation.

The airspeed changes about 23m/s while the aircraft is in a nose down position which is very close to the real data as this was 20m/s when the elevator was released during flight. It also increases in similar magnitude as when the pitch attitude was increasing, the airspeed increased by approximately 45m/s for Simulink and 43m/s for real life data.

4.1.3 Dutch Roll

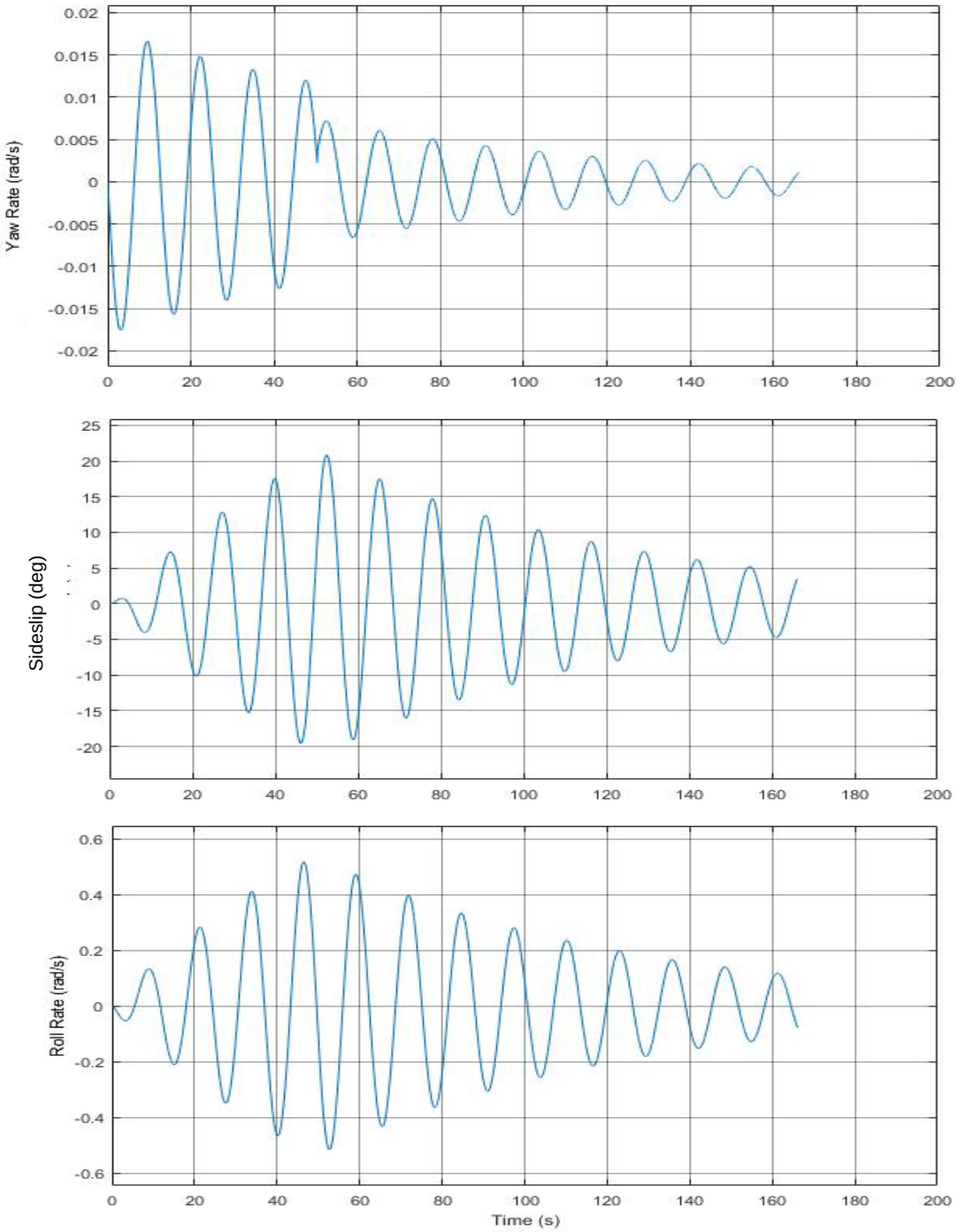

Figure 14: Dutch roll response from Simulink

The graph produced from Simulink for yaw rate shows oscillation but is not the same shape as it should diverge then converge whereas the Simulink one just converges. However, it shows when the rudder was released near the 50 second mark, the oscillation damps well which follows the same principle as the flight test data results.

Sideslip and roll rate follow correct profiles as they diverge then converge when the rudder is released. However, the magnitudes are slightly different where Simulink made more sideslip and roll rate for the Dutch roll. This may be due to the point of rudder release as for the Simulink it was a little later compared to real test data which would cause the magnitudes to develop more.

The possible cause of the correct shape for sideslip and roll rate but different shape for yaw rate is because yaw rate is directly affected by rudder whereas the sideslip and roll rate a indirectly connected.

5. Comparison

Brief comparisons were made between flight sim data and Simulink data whilst analysing the Simulink data above. To have a singular variable to compare dynamic modes, damping ratio and natural frequency were used. These only work for oscillatory systems therefore does not include spiral or roll mode.

5.1 Natural frequency and damping ratio for real data

In order to ensure that the damping ratios are mathematically accurate, it was necessary to use three separate mathematical methods to calculate three independent ratios. Equations obtained from Blackboard were used to calculate each damping ratio at each mode, using data taken from the graphs. Three extra sources (Nelson, Pradeep, and Cornell) were used to calculate damping ratios, to compare to those calculated via Blackboard. Damping ratios for the short period and phugoid were calculated using Nelson, Pradeep, and Blackboard. However, as Pradeep does not refer to Dutch roll, it was mandatory to discover an additional source to calculate the damping ratio. Cornell was chosen, due to the university's high status as an educational body, and that it involves a contrasting method. Rather than solely using equations, Cornell's method was achieved via the use of a Matrix – with the roots being used to calculate the damping ratio.

Equations used for Short Period:

$$\omega_{nsp} = \sqrt{\frac{Z_\alpha M_q}{u_0} - M_\alpha}$$

$$\zeta_{sp} = -\frac{M_q + M_{\dot{\alpha}} + \frac{Z_\alpha}{u_0}}{2\omega_{nsp}}$$

[Nelson, p. 131]

$$\omega_{sp} = \sqrt{\frac{Z_\alpha M_q - M_\alpha U_1}{U_1}}$$

$$2\zeta_{sp}\omega_{sp} = -\left(M_q + M_{\dot{\alpha}} + \frac{Z_\alpha}{U_1}\right).$$

(14)

[Pradeep, p. 92]

Equations used for Phugoid:

$$\omega_{n_p} = \sqrt{2}\frac{g}{u_0}$$

$$\zeta_p = \frac{1}{\sqrt{2}}\frac{1}{L/D}$$

[Nelson, p.129]

$$\omega_p = \sqrt{\frac{-gZ_u}{U_1}}$$

$$2\zeta_p\omega_p = -X_u.$$

(15)

[Pradeep, p. 95]

Equations used for Dutch roll:

$$\omega_{n_{DR}} = \sqrt{\frac{Y_\beta N_r - N_\beta Y_r + u_0 N_\beta}{u_0}}$$

$$\zeta_{DR} = -\frac{1}{2\omega_{n_{DR}}}\left(\frac{Y_\beta + u_0 N_r}{u_0}\right)$$

[Nelson, p.165]

$$\mathbf{A} = \begin{pmatrix} Y_v & Y_p & g_0 \cos\Theta_0 & Y_r - u_0 \\ L_v & L_p & 0 & L_r \\ 0 & 1 & 0 & 0 \\ N_v & N_p & 0 & N_r \end{pmatrix}$$

$$\zeta_{DR} = \sqrt{\frac{1}{1 + \left(\frac{\eta}{\xi}\right)^2_{DR}}} \quad (16)$$

[Cornell, p. 91]

Table 1: Table showing various damping ratios and frequencies

		SPPO		Phugoid		Dutch roll	
		Pitch rate	AOA	Pitch angle	Speed	Sideslip	Yaw rate
Blackboard	Frequency	1.043118514	1.311826555	0.471089995	0.606135804	-0.187230876	0.380586243
	Damping ratio	0.315118527	0.385323466	0.148294611	0.189445145	-0.059491879	0.120265075
Nelson	Frequency		0.097522115	0.698497177	0.698497177		0.50982674
	Damping ratio		0.445648604	0.148271895	0.148271895		-0.060894487
Pradeep	Frequency		0.097522115		0.698461624	N/A	
	Damping ratio		0.439671103		0.188253721		
Cornell	Frequency						0.543609061
	Damping ratio						0.07755

The table above shows the calculated natural frequencies and damping ratios for Short Period, Phugoid, and Dutch Roll modes.

Frequencies and damping ratios were not calculated for all variable for a number of reasons. First was that we were comparing the values obtained using 3 different methods for one value. Another reason was some formulas were not available to calculate frequencies and ratios in the correct manor.

For the short period mode, the damping ratios, in respect to angle of attack, were calculated using the three separate methods. Both Nelson and Pradeep show a strong correlation in results, with only a 15.66% difference in the calculations. The Blackboard method resulted in a 14.88% difference between the average of Nelson and Pradeep methods. This difference can be explained by the method inaccuracies used by this approach. For example, the responses are taken at large time intervals from each other, reducing the accuracy of the produced data.

However, the frequency response produced by the Blackboard calculations resulted in a 1245.15% difference, compared to Nelson. This, along with the damping ratio difference is

evidence to show that this method is not best suited for the short period role, due to the short cycle time.

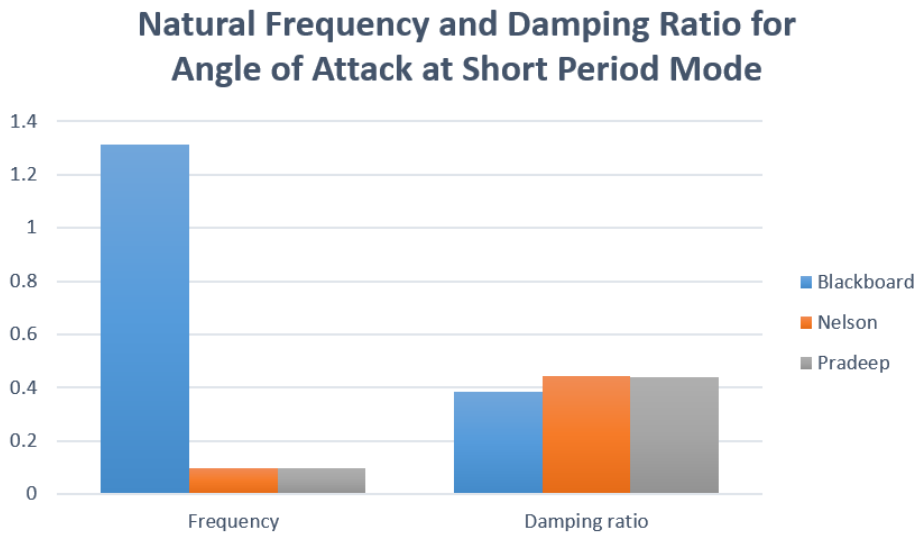

Figure 15: Graph showing natural frequency and damping ratio for AOA for SPPO

The phugoid damping ratios showed more of a correlation between the three methods, with only a 27.77% difference across the three methods. This can be explained due to the longer time. Evidence for this is seen by the decreased difference in the natural frequency, with only a 15.24% difference between the three methods. Both the damping ratio and frequency values are the lowest, out of all the modes calculated. This is due to the longer time of the manoeuvre, and reduces the impact of any individual outliers.

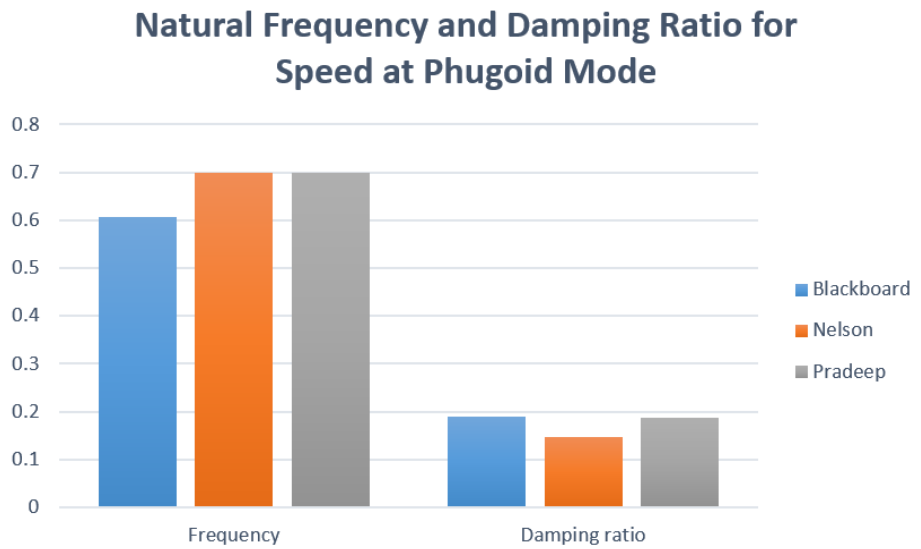

Figure 16: Graph showing natural frequency and damping ratio for speed for phugoid mode

Damping ratios calculated at the Dutch roll mode showed a higher discrepancy, with a 29.49% difference in the results. This, however, is within the error range, and even compared against each other, are evidence for accurate results – validating the results. The difference between the natural frequencies is 42.83%.

Despite this error percentage in both frequency and damping ratio, Nelson predicted the damping ratio as a negative value. This shows that rather than a convergent manoeuvre, the Dutch roll calculated will perform a divergent roll – resulting in an unstable, more turbulent manoeuvre.

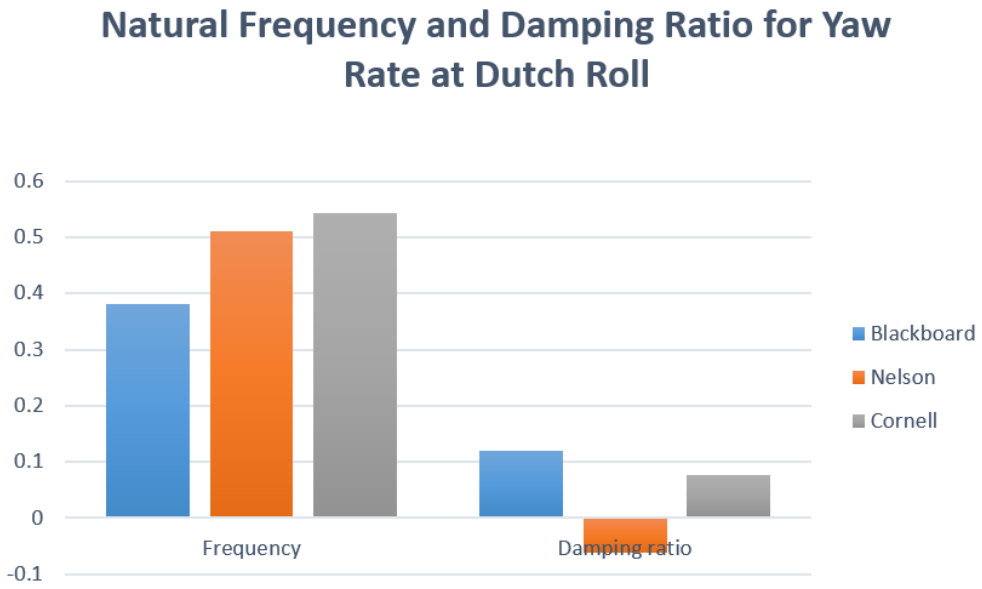

Figure 17: Graph showing natural frequency and damping ratio for yaw rate during Dutch roll

Analysing the results, it is clear to see that the natural frequency that was calculated using Blackboard is significantly lower than those calculated using other sources. This is a result of the Blackboard method being less accurate than any of the mathematical methods that are used.

The phugoid mode contains the most correlated values, due to it' s longer time period and lower amount of damping.

The Dutch roll contains the least correlated results, in both natural frequency and damping ratio. This is due to the sporadic nature of the Dutch roll, as the aircraft's motion can vary greatly.

5.2 Natural frequency and damping ratio from Simulink

	SPPO	Phugoid	Dutch Roll
Natural Frequency	6.9498	0.0063237	-0.0038835
Damping Ratio	0.144	0.0158	-0.001236156

The values above are quite far off from those obtained from real flight test data. This could be for a number of reasons. First is rounding error which could play main role in the inaccuracies. These values were mostly calculated using MATLAB functions. Therefore the code had to be precise to give proximate values.

However, the phugoid values are the closest much like they are seen in the real life data. This could be potentially due to the number of available variables to calculate values.

6. Conclusion

The values taken from the Simulink models ultimately did not closely reflect the values of the calculated predictions. This may be due to inaccurate Simulink models, inaccurate predictions, or a combination of the two.

The MATLAB values could be improved by increasing the significant figures of the values, therefore increasing the accuracy. Alternatively, a more complex simulation could be created – which would model the aircraft in greater fidelity.

A number of the theoretical values could be improved by increasing the sample pool that is used to calculate the averages – resulting in a more representative average, and one less influenced by outliers.

It is also possible that errors are present in both the mathematical predictions, as well as the MATLAB coding and Simulink model.

Future improvements that could be made for this investigation is further statistical analysis of natural frequencies and damping ratios. Better calculations for the ratios and frequencies could be made by further research into the relevant data. Simulink models could be improved by correct variable supplied from the aircraft manufacturer which could make a drastic difference.

7. References

[1] British Aerospace Jetstream (2016) *Wikipedia* [online]. 30 November. Available from: https://en.wikipedia.org/wiki/British_Aerospace_Jetstream [Accessed 1 Novbember 2016].

[2] Flight Test (2015) *Wikipedia* [online]. 28 September. Available from: https://en.wikipedia.org/wiki/Flight_test [Accessed 1 November].

[3] Cranfield University (unknown) *Flight Laboratory Course Handbook*. United Kingdom: Cranfield University, NFLC.

[4] Nelson, R. (1989) *Flight Stability and Automatic Control*. 1st Edition. United States: McGraw-Hill, Inc.

[5] Pradeep, S. (1998) *A century of phugoid approximations* [online]. Bangalore, India: Department of Aerospace Engineering, Indian Institute of Science. Available from : https://blackboard.uwe.ac.uk/webapps/blackboard/execute/content/file?cmd=view&content_id=_5111229_1&course_id=_270254_1 [Accessed 7 November 2016].

[6] Cornell Univeirty (unknown) *Dynamics of Flight Vehicles*. United States of America: Cornell University.

[7] Cooke, A. (2006) *A Simulation Model of the NFLC Jetstream 31* [online]. College of Aeronautics Report number: 0402. Bedford: Cranfield University. Available from: https://core.ac.uk/download/pdf/9637609.pdf [Accessed 7 November 2016]

8. Appendix

Table 2: Values used for MATLAB code

Value	Symbol	MATLAB notation	Description
11738	I_x	Ix	2nd Moment of Inertia
16628.4	I_y	Iy	2nd Moment of Inertia
25761.61	I_z	Iz	2nd Moment of Inertia
0	CD_u	CDu	Stability Coefficient
0.023	CD_0	CD0	Zero-Lift Drag Coefficient
0.3	CL_0	CL0	Lift Coefficient at 0 Angle of attack
5.19	CL_α	CLa	Lift Coefficient Alpha
6.4	$CL_{\alpha w}$	CLaw	Lift Coefficient Alpha for Wing
3.8682	$CL_{\alpha t}$	CLat	Lift Coefficient Alpha for Tail plane
	C_D	CD	Total Coefficient of Drag
0.2763	D_ε/D_α	DEpsDa	(D_Epsilon)/(D_Alpha)
25.0838	S	S	Wing Area
1.435	Sh	Sh	Height of the Tail plane
1.86	MAC	MAC	Mean Aerodynamic Chord
9.2472	Th	Th	Distance Between Centre of Gravity and Tail plane
10	AR	ARw	Aspect Ratio for the Wing
0.75	e	e	Oswald Efficiency
3.244	η_{u_t}	tailplaneEffFac	Efficiency Factor for the Tail Plane
0.82	η_{u_f}	finEffFac	Efficiency Factor for the Fin
6.604	bH	bH	Tail plane Span
6.604	bE	bE	Elevator Plane
0.8	τ_e	tauE	Elevator Effectiveness Parameter
1.54	$d_{f_{max}}$	fuselageMaxDepth	The Maximum Depth of the Fuselage
1.98	$w_{f_{max}}$	fuselageMaxWidth	The Maximum Width of the Fuselage
13.347		fuselageLength	The Length of the Fuselage
0	Λ	wingSweepAngle	The Angle of wing sweep
4.734	Sv	Sv	Vertical tail planform area
8.69	Iv	lv	The Moment Arm of the Tail plane
0.333	λ	wingTaperRatio	Taper Ratio of the Wing
0.122	Γ	wingDihedralAngle	Dihedral Angle of the Wing (rad)
0	zv	zv	The vertical Distance from the Wing Aerodynamic Centre
26.4114		Sfs	Projected Side of the Fuselage
0.0002	IF	kn	Interference Factor of the Wing-Body
1.5	kRe	kRL	Reynolds Number Correction Factor for the Fuselage

Table 3: Gantt chart

Planned start
Completed as planned
Ran over plan

TASK	PLAN START	PLAN DURATION (weeks)	ACTUAL START	ACTUAL DURATION (weeks)	WEEK STARTING									
					26/09/2016	03/10/2016	10/10/2016	17/10/2016	24/10/2016	31/10/2016	07/11/2016	14/11/2016	21/11/2016	28/11/2016
Cranfield ground school session	26/09/16	1	26/09/16	1										
Cranfield day trip	29/09/16	1	29/09/16	1										
Cranfield debrief	07/10/16	1	07/10/16	1										
Flight data extraction	10/10/16	1	17/10/16	2										
Listing of variables for code	17/10/16	2	17/10/16	2										
MATLAB and Simulink	24/10/16	3	31/10/16	4										
Report - Literature review	31/10/16	1	31/10/16	1										
Report - Methodology	07/11/16	1	14/11/16	1										
Report - Results	14/11/16	2	14/11/16	3										
Report - Comparison	14/11/16	1	21/11/16	1										
Report - Abstract, Conclusion	14/11/16	1	21/11/16	1										
Report - Formatting	28/11/16	1	28/11/16	1										